REVIEW

Check for updates

Controllable synthesis and electrocatalytic applications of atomically precise gold nanoclusters

Qingyi Zhu, Xiaoxiao Huang, Yunchu Zeng, Kai Sun, Linlin Zhou, Yuying Liu, Liang Luo, Shubo Tian* and Xiaoming Sun

Nanoclusters are composed of metal atoms and ligands with sizes up to 2–3 nm. Due to their stability and unique structure, gold nanoclusters with precise atomic numbers have been widely studied. Until now, atomically precise gold nanoclusters have been synthesised by various methods. Common ones include the Brust–Schiffrin method and the size-focusing method. With more detailed research on gold nanoclusters, more novel methods have been adopted to synthesise atomically precise gold nanoclusters, such as anti-galvanic reduction, ligand-exchange reactions from metal nanoclusters, the seed growth method, and so on. Besides, the nanoclusters also have many unique properties in electrochemical catalyses, such as the ORR, OER, *etc.*, which are helpful for the development of the energy and environment. In this review, the synthesis methods and electrochemical applications of atomically accurate gold nanoclusters in recent years are introduced.

1 Introduction

In recent years, metal nanoclusters (NCs) have attracted great interest and have been explored increasingly as a newly developing class of materials. NCs are molecular compounds that combine inorganic and organic components. With their sizes reaching 2–3 nm, they fill the size gap between single atoms and nanoparticles (Fig. 1).[1–3] Due to NCs being highly monodisperse, stable, and structurally well-defined, gold nanoclusters (Au NCs) were among the most popular in atomically precise metal NCs.[4] The research of atomically precise Au NCs is vital for developing various types of nanoclusters and their practical applications.[5] With the deepening of atomically precise Au NC research, the mechanism of the reaction and the relationship between the nanoclusters with ligands protecting the core and the properties of materials are easier to understand.[6] Generally, it is denoted as $Au_x(L)_y$, where x represents the number of Au atoms, and y is the number of ligands protecting the gold core (L).[4] Until now, there have been many reports on the synthesis, and applications of atom-precise Au NCs. Scientists have synthesised dozens of atomically precise Au NCs; commonly encountered ones are $Au_{15}(SR)_{13}$,[7] $Au_{22}(SR)_{18}$,[8] $Au_{25}(SR)_{18}$,[7] $Au_{38}(SR)_{24}$,[9] and $Au_{102}(SR)_{44}$.[10] In addition, they also synthesised atomically precise alloy nanoclusters containing Au atoms, such as $[Au_{10}Ag_2(2\text{-}pyC{\equiv}C)_3(dppy)_6](BF_4)_5$,[11] $[Au_{13}Cu_2(DPPP)_3(SPy)_6]^+$,[12] and so on. Since the

electrons of Au atoms are limited to exist at discrete energy levels, atomically precise Au NCs show various electronic and optical properties,[13] such as strong optical properties,[14,15] magnetism,[16] and high electrocatalytic reactivity.[17]

Controllable synthesis of metal nanoclusters has been in development for a long time after Brust *et al.* first synthesised Au NCs in 1994,[18] and new controllable synthesis methods are still being discovered. Since the first atomically precise metal nanoclusters, $Au_{102}(SR)_{44}$, have been synthesised, more and more Au NCs of atomically precise sizes have been reported, and some of their structures have been determined by X-ray crystallography.[19,20] Because of the strong affinity to the Au core, thiol derivatives are always used as ligands to stabilize nanoclusters.[13] In order to pursue better performance and applications of the nanoclusters, researchers used controllable synthesis to synthesize atomically precise Au NCs. For example, the size of Au NCs can be adjusted by the ligand exchange method. Jin group's reported that $Au_{28}(TBBT)_{20}$ could be synthesised by reacting pure $[Au_{25}(PET)_{18}]^-TOA^+$ with excess TBBT

State Key Laboratory of Chemical Resource Engineering, College of Chemistry, Beijing University of Chemical Technology, Beijing 100029, China. E-mail: tianshubo@mail.buct.edu.cn
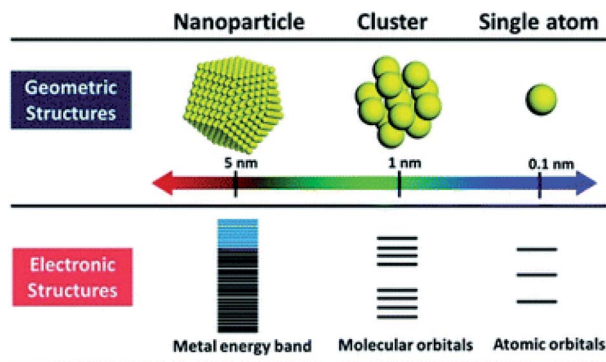
Fig. 1 Size scale from single atoms to nanocrystals.

Fig. 2 Geometric and electronic structure of nanoscale metal materials. Reproduced with permission.[25] Copyright 2018 American Chemical Society.

(TBBT = 4-*tert*-butylbenzenethiolate).[21] Moreover, Au NCs can be alloyed by anti-galvanic reduction.[22] Until now, various synthetic methods and routes have been applied to prepare atomically precise Au NCs successfully.[13]

Atomically precise Au NCs have been applied for electrocatalytic applications. Electrocatalysis focuses on preventing environmental problems consisting of fossil fuel consumption and global warming. To solve environmental problems and achieve energy regeneration and conversion, it is necessary to improve the reaction efficiency of fuel cell reactions, such as the oxygen reduction reaction (ORR), oxygen evolution reaction (OER), hydrogen evolution reaction (HER), and so on.[23] Due to Au NCs having a discrete electronic structure (Fig. 2), it is particular to obtain some novel properties like HOMO–LUMO electronic transition. The unique electronic structures of Au NCs make them efficient electrochemical catalysts.[24,25] Increasing or decreasing one atom of Au NCs often leads to a change in their properties. Hence it is better to clarify the number of Au atoms and ligand types that would be better applied in various electrochemical applications.[26] According to the variety of structures of nanoclusters, atomically precise Au NCs exhibit different excellent electrochemical properties.

This review mainly discusses the controllable synthesis and electrochemical catalytic applications of atomically precise Au NCs. Because of their stability, atomically precise Au NCs are widely studied. Until now, more and more atomically precise Au NCs have been synthesised by various methods. A review of these methods will help us to synthesise the desired Au NCs, and provide ideas for developing new nanoclusters in the future. In addition, atomically precise Au NCs are applied in electrocatalysis, which offers new insights and methods for solving energy and environmental problems.

2 Controllable synthesis methods

2.1. Bottom-up method

On the nanometer scale, small units such as atoms, molecules, and nanoparticles are self-assembled through weak or strong interactions to form relatively large and complex structural systems, which is called the bottom-up method. The Brust–
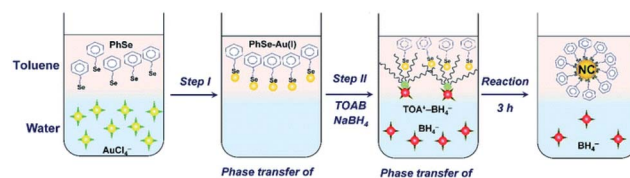

Fig. 3 Schematic diagram of the two-phase synthesis of Au NCs. Reproduced with permission.[27] Copyright 2020 The Royal Society of Chemistry.

Schiffrin method is a typical bottom-up method, which was derived from the synthesis of thiol-protected Au NCs by Brust and co-workers in 1994.[18] Subsequently, the development of Au NC synthesis is rapid; many researchers have employed this method and carried out various modifications on the Brust–Schiffrin methods. It has become the most typical method to synthesise atomically precise Au NCs.

There are two kinds of systems for the Brust–Schiffrin method, the two-phase system and the one-phase system.[13] Among them, the two-phase system is the most widely used. There are two steps in the two-phase system. In step 1, both the Au(III) precursor and the reducing agent like $NaBH_4$ are transferred from the aqueous to the organic phase, and then in step 2, the Au(III) precursor is reduced by the reducing agent and combined with protecting ligands to obtain Au NCs (Fig. 3).[13,27] In the one-phase system, the Au(III) precursor and the reducing agent are in a polar solvent. Brust *et al.* first synthesised Au NCs by a one-phase method; thereafter atomically precise Au NCs were synthesised in a one-phase system.[28] Das *et al.* synthesised $[Au_{23}(c\text{-}C_6)_{16}]^-$ following the one-phase method. The synthesis involved the sodium borohydride ($NaBH_4$) reduction of gold salt, using cyclohexanethiol as the ligand and methanol as the solvent.[29]

After the Brust–Schiffrin method was established, more researchers came up with many modified versions to synthesise atomically precise Au NCs. Toikkanen *et al.* reported monolayer-protected $Au_{38}(SR)_{24}$ nanoclusters. Due to the optimization of the Brust–Schiffrin two-phase synthesis method, $Au_{38}(SR)_{24}$ was fully passivated by the thiol ligands. Based on its stability in the overmuch thiol monolayer, thiol-protected Au_{38} is obtained by controlling the synthesis temperature, and the reduction time resulted in a higher proportion of $Au_{38}(SR)_{24}$ with a uniform core diameter.[30] Dou *et al.* studied the roles of TOAB (TOAB = tetraoctylammonium bromide) in the two-phase Brust–Schiffrin methods, and then they varied the amount of TOAB to control the size of atomically precise Au NCs at the atomic level, such as $Au_{18}(PhSe)_{14}$, $Au_{25}(PhSe)_{18}$, $Au_{23}(PhSe)_{16}$, and $Au_{31}(PhSe)_{20}$.[27] Furthermore, Yang and Chen successfully synthesised $Au_{11}\text{-}Cl_3(PPh_3)_7$ after slight modification of the Brust–Schiffrin method;[31] these nanoclusters exhibit excellent semiconductor electronic properties, and they also observed photoluminescence in the visible range.

2.2. Size-focusing methodology

Controlling the size of nanoclusters with atomic precision has been a significant challenge in molecular chemistry. With the
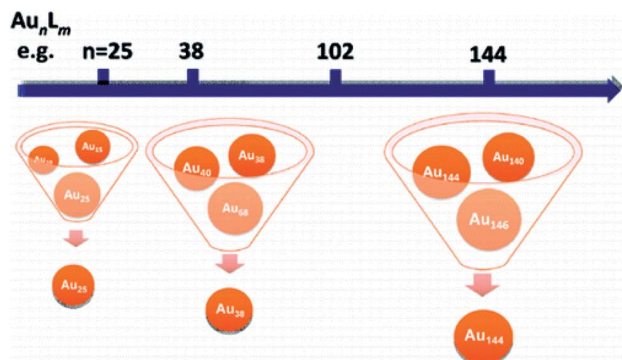
Fig. 4 Scale of the size-focusing methodology. Reproduced with permission.[32] Copyright 2010 American Chemical Society.

development of research in this field, recent studies have increased the probability of preparing atomically precise Au nanoparticles. The size-focusing method is a precise method to design a series of atomic nanoclusters that span the size regimes (Fig. 4),[32] which control the size by adjusting reaction conditions. Interestingly, it is based on "survival of the fittest".[32,33] In addition, Jin *et al.* summarised two critical points about the size-focusing method: one is utilizing the different stabilities of various sized $Au_n(SR)_m$, and another is having an appropriate size distribution of the $Au_n(SR)_m$ mixture for size-focusing.[32]

Even today, there are many kinds of research studies for atomically precise Au NCs synthesised with different atomic numbers. For instance, Das *et al.* reported a cyclohexanethiolate-capped $[Au_{23}(SR)_{16}]^-$ nanocluster, and they prepared pure $[Au_{23}(c\text{-}C_6)_{16}]^-$ nanoclusters *via* the size-focusing method.[29] Qian *et al.* synthesised a $[Au_{25}(PPh_3)_{10}(SC_2H_4Ph)_5Cl_2]^{2+}$ nanocluster by size-focusing conversion; in the presence of phenylethanethiol, polydisperse gold nanoparticles capped by phosphine, and then monodisperse $[Au_{25}(PPh_3)_{10}(SC_2H_4Ph)_5Cl_2]^{2+}$ nanoclusters were obtained.[34] In this work, they identified the crystal structure of $[Au_{25}(PPh_3)_{10}(SC_2H_4Ph)_5Cl_2]^{2+}$ nanoclusters and an important side-product $[Au_2(PR_3)_2(SC_2H_4Ph)]^+$ formed in the size focusing process, the transformation process is more explicit. Liu *et al.* utilized theoretical prediction to synthesise $Au_{36}(SR)_{24}$ nanoclusters;[35] two isomers $Au_{36}(DMBT)_{24}$-1D and $Au_{36}(DMBT)_{24}$-2D in $Au_{36}(SR)_{24}$ were synthesised using a two-step size-focusing method, and DMBT was selected as the protecting ligand. In addition, other atomically precise Au NCs such as Au_{38},[36] Au_{64},[37] and Au_{99} (ref. 38) can also be synthesised by the size-focusing method. It can also be applied in Au–M alloy nanoclusters. For example, Qian *et al.* produced the mixture of
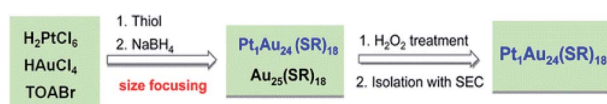
$Pt_1Au_{24}(SC_2H_4Ph)_{18}$ and $Au_{25}(SC_2H_4Ph)_{18}$ *via* a size-focusing process first,[39] and $Pt_1Au_{24}(SC_2H_4Ph)_{18}$ was obtained by further separation and purification (Fig. 5).

2.3. Reduction method

The reduction method is a general method to obtain target products. In the synthesis of atomically precise Au NCs, common reducing agents are carbon monoxide (CO), $NaBH_4$, ascorbic acid, *etc.*

CO is a great reducing agent for Au NC synthesis, and it can produce a gentle reduction environment for the Au ions.[40] Xie and co-workers first utilized CO as a gaseous reducing agent to reduce Au ions in 2012. They followed the growth process of $Au_{25}(SR)_{18}$ and found that CO provided a milder reduction environment as compared to $NaBH_4$.[40] In addition, they used CO to control the reduction, and presented a one-pot synthesis method to produce various discrete-size Au NCs with different thiol ligands such as Au_{10-12}, Au_{15}, Au_{18}, and Au_{25}.[7] In that work, Au^{3+} and glutathione were mixed to obtain Au(I)–SG complexes, then NaOH was added to adjust pH, and CO was then bubbled to transform Au(I) into Au(0). It was found that different pH results in a different number of gold atoms in the product (Fig. 6). In 2014, Xie and co-workers explained the growth mechanism in a CO gaseous reduction environment.[41] It followed a two-stage, bottom-up formation and growth process. The first stage is kinetically controlled growth with CO, and the second stage is thermodynamically held size-focusing growth. Xie's group did much related work for the synthesis of atomically precise Au NCs by CO reduction. For instance, they reported a reversible process for the transformation between $[Au_{25}SR_{18}]^-$ and $[Au_{25}SR_{19}]^0$, using oxidative etching and CO reduction.[42] In addition, Hwang *et al.* also generated Au_{25} with different ligands by CO reduction.[43] It implies that this method has a wide range of applications, producing nanoclusters with different numbers of gold atoms and different ligands. Alloy nanoclusters also can be generated by CO reduction. Xie and co-workers reported the synthesis of thiolate-protected $(AuAg)_{18}$ nanoclusters by adopting the CO-reduction method;[44] these AuAg nanoclusters show great optical and electrical properties.

Since Brust *et al.* synthesised the first Au nanoparticles,[18] $NaBH_4$ is considered the classic reductant. It was adopted by

Fig. 5 Procedure for $Pt_1Au_{24}(SR)_{18}$ synthesis. Reproduced with permission.[39] Copyright 2012 American Chemical Society.
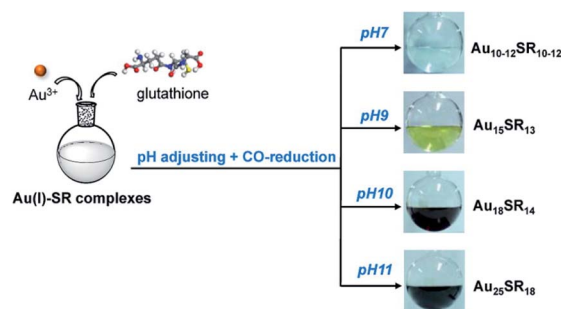

Fig. 6 Size-controlled synthesis of aqueous nanoclusters through pH control. Reproduced with permission.[7] Copyright 2013 American Chemical Society.

most researchers in the later synthesis of atomically precise Au NCs. For example, $[Au_{25}(SNap)_{18}]^{-}[TOA]^{+}$ (SNap = 1-naphthalenethiolate and TOA = tetraoctylammonium), was synthesised by Jin et al.,[45] and is an aromatic-thiolate-protected Au NC. In this reaction, after $NaBH_4$ was added to the solution, the solution turned dark, which showed that Au(I) had reduced to Au(0). In addition, Jin's group also synthesised different sized Au NCs selectively by a controlled reduction method,[46] where the reduction agent used was $NaBH_4$. They have identified that $NaBH_4$ plays a vital role in the size control of the nanocluster. Through tuning the speed of $NaBH_4$ addition during the step of Au(I) reduction to nanoclusters, different size Au NCs such as $Au_{20}(SC_2H_4Ph)_{16}$, $Au_{24}(SC_2H_4Ph)_{20}$, $Au_{39}(SC_2H_4Ph)_{29}$, and $Au_{40}(SC_2H_4Ph)_{30}$ could be synthesised. Therefore, $NaBH_4$ can participate in the synthesis of nanoclusters with different precise Au atoms, such as Au_8,[47] Au_{10},[48] Au_{13},[49] Au_{18},[50] Au_{25},[51] $Au_{44}(PhC{\equiv}C)_{28}$,[52] and Au_8Ag_3.[53]

Other reducing agents also can be applied to synthesise atomically precise Au NCs. For example, ascorbic acid is a mild biological reductant,[54] Martinez's group demonstrated the synthesis of Au_{13} and Au_{17} by using ascorbic acid as a reducing agent. They prepared Au NCs by using poly(amidoamine) (PAMAM) dendrimers as templates, and produced Au NCs which are stable in a pH range of 6–8. Koyakutty et al. reported fluorescent Au_{25} nanoclusters synthesised by a controlled reduction process.[55] They used ascorbic acid to reduce Au^+ and stabilised nanoclusters by utilizing bovine serum albumin (BSA). Besides ascorbic acid, histidine is another green reducing agent; Chen et al. synthesised Au_{10} nanoclusters, which are water-soluble and monodispersed;[56] in this reaction, histidine was used both as a reducing agent and a protecting ligand. They found that the product Au_{10} nanoclusters had excellent biocompatibility, which had the potential to be applied as future biosensors. Moreover, Me_3NBH_3 (ref. 57) and meso-2,3-dimercaptosuccinic acid[58] also exhibited mild reducing ability, and they were also used to synthesise atomically precise Au NCs.

2.4. Inducement method

The inducement method is a method to synthesise nanoclusters by condition control. The conditions include but not limited to metal addition and heating. The specific methods are described below.

The method of ligand-exchange reactions from metal nanoclusters is one of the inducement methods. It involves introducing new ligands onto original nanoclusters to obtain another new nanocluster,[59] where new properties and functions can be obtained, such as optical properties.[60,61] Negishi et al. reported the first comparison between two Au_{25} nanoclusters with different ligands in 2011.[62] They found that $[Au_{25}(SeC_8H_{17})_{18}]^-$ and $[Au_{25}(SC_8H_{17})_{18}]^-$ have similar geometric structures, but different properties. In recent years, there have already been many studies on the ligand exchange reactions of Au NCs. They not only research the exchange sites deeply,[59] but also propose a clear associative mechanism.[63] The method of ligand-exchange reactions from metal nanoclusters has become a relatively mature method.

Ligand-exchange reactions can control the size of nanoclusters which are difficult to synthesise. In ligand–exchange reactions, there are three kinds of reactions.[65] In the first kind of reaction, the nanoclusters' size decreased. Song et al. reported the size transformation from $[Au_{25}(SePh)_{18}]^-$ to $[Au_{23}(SePh)_{16}]^-$ by a ligand-exchange reaction, where $NaBH_4$ removed two units of "Au-SePh".[64] $[Au_{23}(SePh)_{16}]^-$ also can be transformed into $[Au_{25}(PET)_{18}]^-$ nanoclusters (PET = SCH_2CH_2Ph) with excess PET (Fig. 7). In the second kind of reaction, the nanoclusters' size increased. Wang et al. reported the transformation of $[Au_{25}(SR)_{18}]^0$ into $Au_{28}(SR)_{21}$ with a chiral ligand (S-2-phenyl-propane-1-thiol).[64] In the third kind of reaction, there are ligands exchanged without size change. For instance, Thomas W. Ni et al. presented $Au_{25}(PET)_{16}(pBBT)_2$ (pBBT = p-bromobenzenethiol) from the ligand exchange reaction of $Au_{25}(PET)_{18}$ with pBBT.[63] Stefan Knoppe et al. reported the ligand exchange reaction for $Au_{38}(2\text{-}PET)_{24}$ and $Au_{40}(2\text{-}PET)_{24}$ (2-PET = 2-phenylethanethiol) nanoclusters; the ligand exchange reaction occurred between $Au_{38}(2\text{-}PET)_{24}/Au_{40}(2\text{-}PET)_{24}$ and enantiopure BINAS (BINAS = 1,1'-binaphthyl-2,2'-dithiol), and new nanoclusters were obtained.[66] In addition, this method is also applicable to synthesise alloy Au NCs with precise atoms. Niihori et al. changed phenylethanethiolate-protected Au_{25} nanoclusters into alloy nanoclusters by incorporating Ag or Cu.[67] Using octanethiol ($C_8H_{17}SH$) as the exchange ligand, they synthesised $Au_{25-x}M_x(SC_2H_4Ph)_{18}$ (M = Au, Ag, Cu, or Pd).

Precursor- or ligand-induced etching of metal nanoparticles is another inducement method. Since the formation process of nanoclusters is dynamically balanced, it is crucial to control the growth and etching process of nanocluster formation. It is a good method to prepare atomically precise Au NCs with well-controlled properties of nanoparticles by precursor- or ligand-induced etching of metal nanoparticles.[13,51]

There are two kinds of methods to etch metal nanoparticles, one is the precursor-induced etching of metal nanoparticles; for example, Zhou et al. reported an etching strategy for synthesising Au_8 nanoclusters where the precursors are gold nanoparticles,[68] and the etching process was performed by employing amino acids and peptides as etching agents. Au_8 was characterised by photoluminescence, electrospray ionization mass spectrometry, etc.; Au_8 also shows vast potential in biological imaging and sensors.
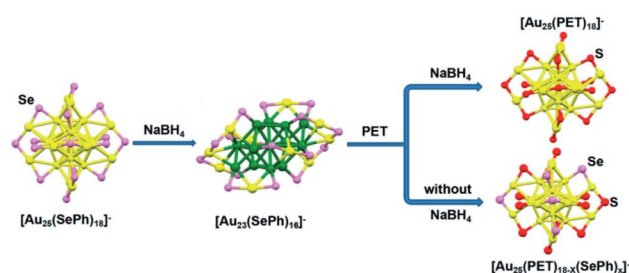

Fig. 7 Conversion from $[Au_{25}(SePh)_{18}]^-$ to $[Au_{23}(SePh)_{16}]^-$, and the asprepared $[Au_{23}(SePh)_{16}]^-$ nanoclusters converted into $[Au_{25}(PET)_{18}]^-$ and $[Au_{25}(PET)_{18-x}(SePh)_x]^-$ with excess PET under different conditions. Reproduced with permission.[64] Copyright 2017 American Chemical Society.
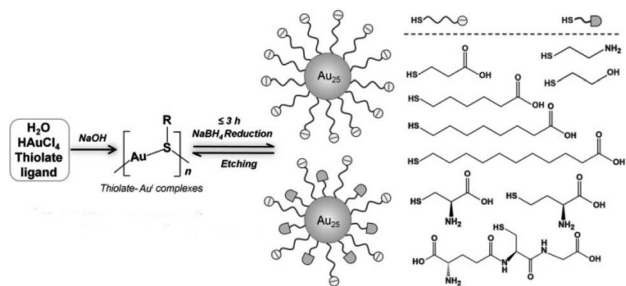
Fig. 8 NaOH-mediated $NaBH_4$ reduction method for the synthesis of Au_{25} NCs. Reproduced with permission.[51] Copyright 2014 Wiley-VCH.

Fig. 9 Synthesis of $Au_{24}Cd_1$ and $Au_{24}Hg_1$ nanoclusters by the AGR method. Reproduced with permission.[76] Copyright 2015 American Chemical Society.

Another method is the ligand-induced etching of metal nanoparticles. Atomically precise Au NCs can be synthesised using the etching capacity of some ligands. Due to the stabilization of nanoclusters in solution, surface atoms of the metallic nanoparticles will be removed to form more stable nanoclusters.[69] For instance, Xie's group reported a strategy to synthesise Au_{25} nanoclusters using a $NaBH_4$ reduction method.[51] Au_{25} NCs formed by decreasing the reduction ability of $NaBH_4$ and increasing the etching ability of free thiolate ligands to balance the reversible reaction (Fig. 8). Duan et al. reported a ligand-induced etching process to prepare water-soluble metal nanoclusters Au_8.[70] They used multivalent coordinating polymers like polyethylenimine to etch preformed colloidal gold nanocrystals, and then atomically precise Au NCs were obtained by reducing agents such as $NaBH_4$. Electrospray ionization mass spectrometry (ESI-MS) data indicated that the nanocluster is Au_8. Chen et al. reported the ligand-induced etching process to transform gold nanoparticles into organic-soluble Au_8,[71] which is different from Duan's method. This illustrates the wide applicability of the ligand-etching method. In addition, Bain et al. utilised a core-etching process to synthesise luminescent Au NCs,[72] Au_6 and Au_8, from Au nanoparticles with excess glutathione ligand. The mixture of $Au_6(SG)_4$, $Au_8(SG)_4$, $Au_6(SG)_2$, and $Au_8(SG)_2$ nanoclusters was shown by mass spectrometric analysis and gel electrophoresis.

An electrochemical reaction occurs when the potential difference between two metals exists; at the same time, the anode with a high potential is oxidized, which is known as the galvanic reaction (GR). However, Wu's group discovered a phenomenon in 2012 which suggests that metal ions can be reduced by less reactive metals.[73] It is clear from the electrochemical potential that the activity of gold is less than that of silver, but they found that Ag ions were reduced by $Au_{25}(SC_2H_4Ph)_{18}$, and the silver atoms replaced several gold atoms in Au_{25}. This is contrary to electrochemical theory. Therefore they named this reaction anti-galvanic reduction (AGR). AGR, which is the opposite of GR,[73] is a general method to prepare alloyed nanoclusters, and it can be used to tune nanoclusters' compositions, structures, and properties.[74]

Ever since Wu and co-workers discovered this reaction, plenty of alloyed nanoclusters have been prepared by using this method. According to the type of alloyed atomically pre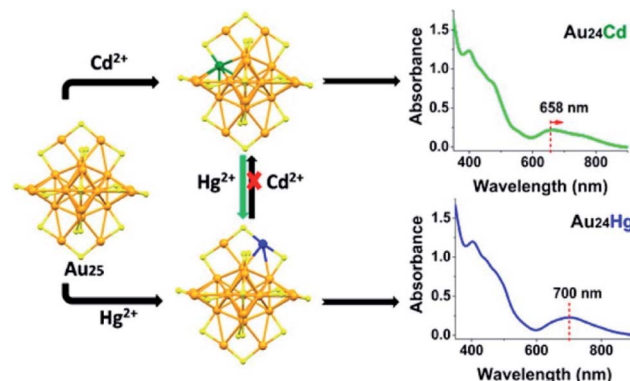cise nanocluster, they divided the methods into three modes;[74] the first one is introducing heteroatoms on existing atomically precise Au NCs. For example, $Au_{25}Ag_2(SC_2H_4Ph)_{18}$ is synthesised by adding two silver atoms on the precursor nanoclusters $Au_{25}(SC_2H_4Ph)_{18}$.[75] The second one is replacing gold atoms of the precursor nanoclusters with heteroatoms, while maintaining the same number of total atoms. Wu's group revealed that Au_{24} Cd and $Au_{24}Hg$ were also produced successfully via AGR with metal thiolate complexes of Cd(II) and Hg(II) (Fig. 9).[76] The third one is introducing heteroatoms which change the number of metal atoms and the structure of nanoclusters to form new precise Au NCs. Wu's group presented a two-phase AGR method to tailor different kinds of Au NCs. For instance, they doped Cd into $Au_{44}(TBBT)_{28}$ to produce $Au_{47}Cd_2(TBBT)_{31}$ nanoclusters;[77] $Au_{25}(SCH_2CH_2Ph)_{18}$ can be transformed into $[Au_{13}Cd_2(PPh_3)_6(SC_2H_4Ph)_6(NO_3)_2]_2Cd(NO_3)_4$.[78] In addition, Zhu's group reported that $Cd_1Au_{24}(SR)_{18}$ and $Hg_1Au_{24}(SR)_{18}$ can be obtained with complexes of Cd^{II} and Hg^{II} by a metal exchange method.[79]

The seed-mediated growth method always occurs in nanoparticle synthesis, but is challenging to apply in nanocluster synthesis. Researchers extended precise reaction routes to synthesise atomically precise nanoclusters in nanochemistry with extensive research in the precise nanoclusters field. In 2006, Tsukuda et al. synthesised a series of Au NCs ranging from 1.3 to 10 nm by seed-mediated growth. Seed nanoclusters were produced by reducing $AuCl^-$ with $NaBH_4$ in poly(N-vinyl-2-pyrrolidone) (PVP),[80] and then a series of size-selective Au NCs are prepared by reducing $AuCl^-$ with Na_2SO_3 in the presence of the seed nanocluster solution. Xie's group prepared Au_{44} from pure Au_{25} nanoclusters by the seed-mediated growth method (Fig. 10) and proposed its mechanism. They came up with a mechanism containing three steps.[81] Firstly, the seed nanocluster Au_{25} accumulates according to kinetics, where Au_{25} was synthesised by the CO reduction method. Secondly, the size of Au_{25} increased, and thirdly, Au_{44} is obtained by the size-focusing method, which is thermodynamically controlled. Comparing Fig. 10b, d and Fig. 10c, e, in which the characteristic peaks corresponding to Au_{25} and Au_{44} are observed, indicated that Au_{44} was produced. Similarly, they also synthesised
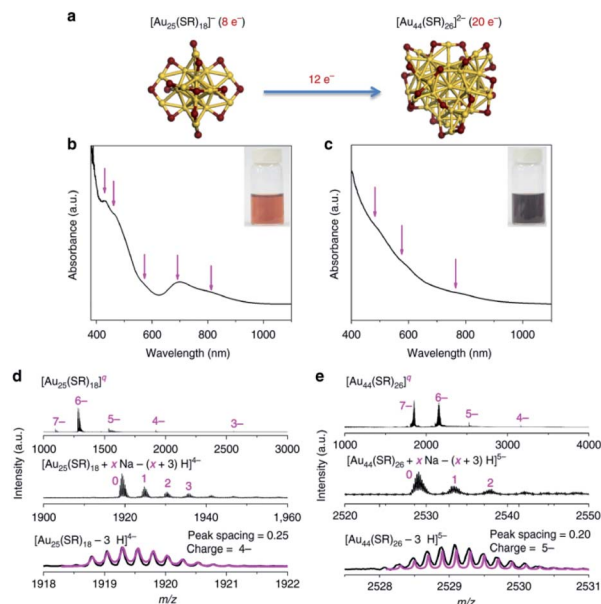
Fig. 10 (a) Schematic illustration of the size growth reaction from $[Au_{25}(SR)_{18}]^-$ to $[Au_{44}(SR)_{26}]^{2-}$ (yellow, Au; purple, S). (b and c) Ultraviolet-visible absorption and (d and e) electrospray ionization mass spectrometry spectra of (b and d) $[Au_{25}(SR)_{18}]^-$ and (c and e) $[Au_{44}(SR)_{26}]^{2-}$. Reproduced with permission.[81] Copyright 2017 Nature Publishing group.

$Au_{38}(SR)_{24}$ based on the mechanism of the seed-mediated growth method. The above results suggest that the seed-mediated growth method for nanocluster synthesis overcame the bottleneck in precisely customizing structural attributes.

The thermal transformation method is always applied to produce nanoclusters with high thermal stability. Jin's group indicated that pure $Au_{38}(SC_2H_4Ph)_{24}$ nanoclusters can be separated from a distribution of Au NCs, by thermal thiol etching for ∼30 h.[82] First they obtained a mix of $Au_{25}(SC_2H_4Ph)_{18}$ and $Au_{38}(SC_2H_4Ph)_{24}$ via the size-focusing method from the crude product, and then the crude product was isolated. $Au_{25}(SC_2H_4Ph)_{18}$ nanoclusters were produced after aging at room temperature. However, $Au_{38}(SC_2H_4Ph)_{24}$ nanoclusters were obtained by another approach, where the crude product was further subjected to thermal thiol etching in a toluene solution.

Pure $Au_{38}(SC_2H_4Ph)_{24}$ nanoclusters could be obtained. It is indicated that these two kinds of nanoclusters can be synthesised in different environments. On this basis, Jin et al. synthesised $Au_{38}(SR)_{24}$ with different ligands via the thermal transformation method.[36] In this work, a crude mixture containing glutathionate-capped $Au_n(SG)_m$ nanoclusters was subjected to the thermal thiol exchange process, which led to the exchange of SG to $SC_{12}H_{25}$ in a two-phase system. Finally, the polydisperse nanoclusters converted to $Au_{38}(SC_{12}H_{25})_{24}$ nanoclusters with high purity.

In addition, other different atomically precise Au NCs can also be produced by the thermal transformation method. For example, Jin's group found that $Au_{38}(SCH_2CH_2Ph)_{24}$ can also be transformed into $Au_{36}(SPh\text{-}tBu)_{24}$ by reacting with HSPh-tBu at 80 °C.[83] They also synthesised $Au_{28}(TBBT)_{20}$ nanoclusters, $[Au_{25}(PET)_{18}]^- TOA^+$ by reacting with excess TBBT thiolate at 80 °C.[21] After several hours, the $Au_{25}(PET)_{18}$ nanoclusters were converted to $Au_{28}(TBBT)_{20}$ in high yield with almost no by-products.

2.5. Template-based synthesis methods

The template-based synthesis method is an essential method for the synthesis of nanomaterials and is also the most widely used method in nanomaterial research, especially for the preparation of nanomaterials with specific properties. With a precise number of atoms and overall molecular composition, atomically precise Au NCs have unique atomic packing. They have particular structure patterns so that the nanoclusters exhibit different properties, such as catalytic activity.[84] Thus, template-based synthesis methods can design the atomically precise Au NCs according to the performance requirements.

Until now, many macromolecules such as dendrimers, peptides, and proteins have been chosen as templates. According to different properties and applications, the atomically precise Au NCs are synthesised in unique ways.[13] Tsukamoto et al. worked on a series of new atomically precise nanoclusters composed of five elements ($Ga_1In_1Au_3Bi_2Sn_6$),[85] which adopted the template-based synthesis method. The phenylazomethine dendrimer is used as a macromolecular template, and the size and composition of the alloyed nanoclusters can be precisely controlled by controlling the metal precursor complexes. Lv et al. first reported self-assembling tripeptides as reducing soft templates to synthesise atomically precise Au NCs, and the resulting fluorescent Au NCs on the soft template were applied to bio-imaging.[86] Three tripeptides are self-assembled to form soft templates with different morphologies using cryogenic treatment. The size of Au NCs is determined by the distribution of the –SH sites on the template. Landman's group utilised proteins to obtain Au_{25}^+, Au_{38}^+ and Au_{102}^+.[84] These atomically precise Au NCs can be electronically stabilised in the protein, forming electronic closed-shell structures, which enhanced the stability of the Au NCs. Generally speaking, template-based synthesis methods allow different templates to be easily combined with Au NCs at the sub-nanometre scale to create new materials for actual needs.

3 Electrocatalytic applications

With "carbon-neutral" trends on the rise, hydrogen energy will occupy an important position in the future due to its renewable and efficient characteristics. Fuel cells convert chemical energy of fuels into electrical energy. Advantages of fuel cells include unlimited sources of reactants and no environmental pollution. Due to the rapid depletion of fossil fuel consumption, fuel cell technology has become an alternative technology for efficient energy conversion and storage.[87,88] At present, electrocatalytic applications of atomically precise Au NCs include but are not limited to the oxygen reduction reaction (ORR), oxygen evolution reaction (OER), hydrogen evolution reaction (HER), carbon

dioxide reduction reaction (CO_2RR), and nitrogen reduction reaction (N_2RR).

3.1. ORR

The ORR is a four- or two-electron reaction, at the cathode of a proton exchange membrane fuel cell, where oxygen is reduced by the reaction with protons and electrons to produce water ($1/2 O_2 + 2H^+ + 2e^- \rightarrow H_2O$).[87,89] In general, platinum-based catalysts are chosen to achieve excellent fuel cell performance; however, Pt is expensive.[87] Recently, research has showed that Au NCs could also exhibit good performance in the ORR. For example, Chen *et al.* used Au_{25}, Au_{38}, and Au_{144} nanoclusters to prepare porous carbon-supported gold nanoparticles.[88] They found that the nanoparticles prepared with Au_{25} nanoclusters exhibited the best activity, with the positive onset potential at +0.95 V *vs.* the reversible hydrogen electrode (RHE) and electron transfer at potentials from +0.50 to +0.80 V is high. In addition, they also prepared porous carbon nanosheets based on *p*-mercaptobenzoic acid-functionalized Au NCs, Au_{102}(*p*-MBA)$_{44}$,[90] and used this catalyst to test the performance of the ORR. 30% Au mass loading was found to be optimal, as manifested by the onset potential at +0.96 V and diffusion-limited currents (at +0.55 V) reached 4.20 mA cm^{-2} for Au CNs-30% (Fig. 11). The performance of both catalysts were comparable to that of commercial Pt/C. Chakraborty's group also investigated the ORR of Au_{28}, Au_{36}, Au_{133}, and Au_{279}.[91] They found that Au_{36}(SCH$_2$CH$_2$Ph)$_{24}$ is the most active molecule for the ORR, as shown by the over-potential of 160 mV and quantitatively yielding the $4e^-$ reduced product OH^-. These above results demonstrated that the materials based on precise atomically Au NCs can be high-efficiency ORR catalysts.

3.2. OER

Nowadays, research on electrochemical catalysts for the OER with good stability, efficiency and low cost is a top concern in industry.[92] At present, noble metals such as ruthenium (Ru), iridium (Ir), and platinum (Pt) are the most common OER catalysts.[93] What is exciting is that Au NCs with particular atoms also possess excellent properties. Negishi's group found that $[Au_{24}Pd(PET)_{18}]^0$ can act as a OER catalyst with high potential. These findings provide guidelines to design $Au_n(L)_m$ nanoclusters as highly active OER catalysts.[94]

Su *et al.* proposed to load Au_{13} in $Ni_{120}P_{50}$ for the OER test.[95] The results of the OER test were compared with that of Au nanoparticles which were loaded on $Ni_{12}P_5$. It is found that the OER performance of $Au_{13}@Ni_{120}P_{50}$ is better than that of $Ni_{12}P_5$ (001) supported by Au. The kinetic energy barrier of $Au_{13}@Ni_{120}P_{50}$ is 2.18 eV, which is lower than the 3.168 eV of $Ni_{12}P_5$ (001) supported by bulk Au. The lower thermodynamic overpotential and kinetic energy barrier confer $Au_{13}@Ni_{120}P_{50}$ a significant position as an OER electrocatalyst. Jin's group constructed Au_n/$CoSe_2$ composites for electrocatalytic water oxidation,[96] where Au_n represents Au_{25}(SR)$_{18}$, Au_{144}(SR)$_{60}$, and Au_{333}(SR)$_{79}$ nanoclusters (where R = –CH$_2$CH$_2$Ph); they found that the OER activity and durability of the Au_n/$CoSe_2$ composites in the alkaline electrolyte are high, and the overpotential of Au_{25}/$CoSe_2$ was found to be 0.43 V at 10 mA cm^{-2} which is better than that of $CoSe_2$ (0.52 V). The results exhibited that Au NCs can be utilised to improve the catalytic performance for the OER. In summary, atomically precise Au NCs can be used to develop highly efficient nanocatalysis for the OER.[97]

3.3. HER

The HER is an ideal pathway to produce hydrogen. It has the advantages of abundant raw materials and no pollution to the environment. So far, researchers have reported a number of HER catalysts with excellent performance, even some performance exceeding that of commercially available Pt/C catalysts.[98–100]

However, there is much to be explained about the interaction between hydrogen and metals for these catalysts. Atomically precise Au NCs provide an ideal template for the mechanism of the HER reaction. Jiang *et al.* studied the interaction of hydrogen with $[Au_{25}(SR)_{18}]^q$ and single atom doped bimetallic $[MAu_{24}(SR)_{18}]^q$ (M = Pt, Pd, Ag, Cu, Hg or Cd).[101] They found that hydrogen behaves like a metal in nanoclusters and contributes its 1s electrons to the number of superatomic free electrons. Doping other metals can increase the HER performance. For instance, Lee's group doped Pt and Pd atoms into stable Au NCs to control the catalysts' electronic structure and catalytic activity.[102,103] The results showed that the doped Au NCs have a higher catalytic current and TOF, which decreases in the order of $PtAu_{24}$ > $PdAu_{24}$ > Au_{25}. The same trend was also observed in Au_{38} nanoclusters (Pt_2Au_{36} > Pd_2Au_{36} > Au_{38}). DFT calculations revealed that the metal doping significantly decreases the hydrogen adsorption free energy (ΔG_H), which indicates the critical role of dopants.

In addition, to improve the performance of the catalysts, Au NCs with precise atoms can also be combined with other materials. For example, Jin's team built a new nanocomposite Au_{25}/MoS_2.[104] Compared to MoS_2 nanosheets, Au_{25}/MoS_2 has
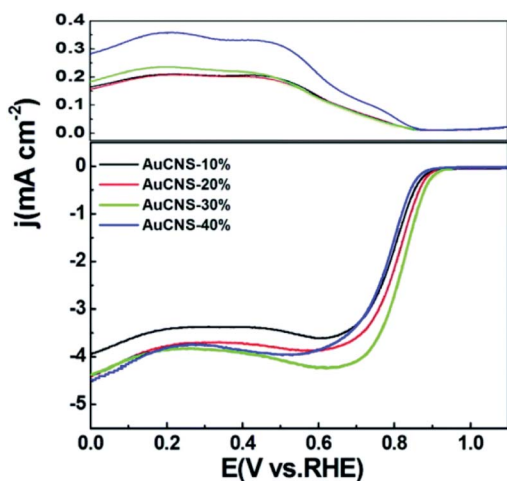

Fig. 11 RRDE voltammogram measurements of AuCNS-10%, AuCNS-20%, AuCNS-30%, and AuCNS-40%, in O_2-saturated 0.1 M KOH at 2500 rpm. Reproduced with permission.[90] Copyright 2013 The Royal Society of Chemistry.

enhanced HER activity, as revealed by a smaller onset potential of 0.20 V (vs. RHE) and a higher current density of 59.3 mA cm^{-2} at a potential of 0.4 V. Zhu's group modified MoS$_2$ with Au$_2$Pd$_6$ nanoclusters.[105] Significantly enhanced HER activity was also observed with a 91 mV positive shift of the onset potential and 31% decrease of the Tafel slope. According to the above analysis, we find that Au NCs are not only used as HER catalysts but also, more importantly, as an ideal template due their well-defined structure and precise composition for researching the relationship between the structure and activity.

3.4. CO$_2$RR

The increase in CO$_2$ emission has led to the worsening of environmental pollution. The CO$_2$RR, as a route of electrocatalysis, can reduce CO$_2$ emissions by converting CO$_2$ to other valuable chemicals and fuels.[107] It has been reported that Au-based materials show high selectivity towards CO formation because the *CO intermediates on gold are relatively weak.[108] Hence, atomically precise Au NCs have been studied extensively on the CO$_2$RR and show excellent performance.

Jin's group studied the interaction between CO$_2$ and Au$_{25}$,[109] and revealed a reversible Au$_{25}$–CO$_2$ interaction through spectroscopic and electrochemical methods. Au$_{25}$ was found to have promoted the conversion of CO$_2$ to CO within 90 mV of the formal potential, which showed that Au$_{25}$ is superior to Au nanoparticles and bulk Au by 200–300 mV. Zhu et al. reported the CO$_2$RR of three Au$_n$ nanoclusters, Au$_9$, Au$_{11}$, and Au$_{36}$.[110] After subjecting the three nanoclusters to the CO$_2$RR, different target products were produced. Methane was produced with Au$_9$, ethanol with Au$_{11}$, and formic acid with Au$_{36}$. As the selectivity of these products exceeded 80%, it showed that there are three kinds of reaction pathways for atomically Au NCs of different sizes. The results revealed that the catalytic performances of Au$_9$, Au$_{11}$, and Au$_{36}$ are atomically dependent. Therefore they can selectively choose the reaction pathways towards C1 or C2 products. In addition, Lee et al. discovered that Au$_{25}$, Au$_{38}$, and Au$_{144}$ nanoclusters exhibited size-dependent activities for the CO$_2$RR,[111] and the selectivity for CO production exceeded 90%. They revealed that dethiolated Au sites are the active sites, and CO$_2$RR activity was determined by the number of active sites on the surface of the nanoclusters. This finding provides insights into the electrocatalysis field, and atomically accurate nanoclusters will become a powerful model for developing properly designed catalysts for the CO$_2$RR.

Similarly, alloy nanoclusters also play an essential role in the CO$_2$RR. For instance, Wu's group prepared Au$_{47}$Cd$_2$(TBBT)$_{31}$ (TBBT = 4-tert-butylbenzenethiolate) nanoclusters by tailoring Au$_{44}$(TBBT)$_{28}$ precisely,[106] before testing and comparing the CO$_2$RR performance. The onset potential of Au$_{47}$Cd$_2$(TBBT)$_{31}$ is much lower than those of the Au$_{44}$(TBBT)$_{28}$ and Au NPs. The Faradaic efficiencies of Au$_{47}$Cd$_2$(TBBT)$_{31}$ increased to 96% at −0.57 V for the electrocatalytic reduction of CO$_2$ to CO (Fig. 12a and b), and the results showed that the partial current density of CO for Au$_{47}$Cd$_2$(TBBT)$_{31}$ is more negative than that of the Au$_{44}$(TBBT)$_{28}$ nanocluster and the Au NPs (Fig. 12c and d) showed that the electrocatalytic durability of Au$_{47}$Cd$_2$(TBBT)$_{31}$

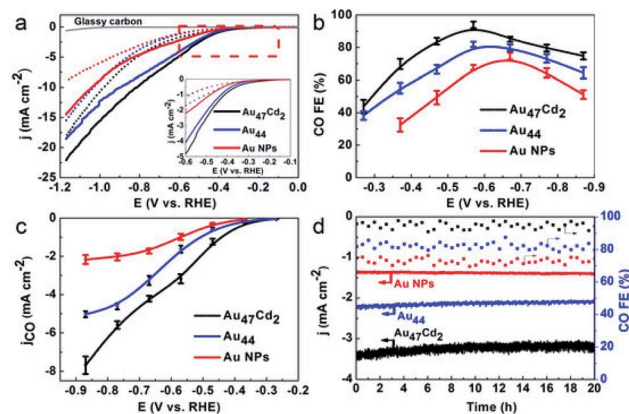Fig. 12 (a) LSV curves of Au$_{47}$Cd$_2$(TBBT)$_{31}$, Au$_{44}$(TBBT)$_{28}$ and the ca.1.5 nm Au NPs in an Ar-saturated (dotted line) and a CO$_2$-saturated (full line) 0.5 m KHCO$_3$ solution; inset: enlarged LSV curves from @0.1 V to @0.6 V. (b) CO faradaic efficiency for the catalysts examined with different applied potentials. (c) The corresponding CO partial current density. (d) The stability test conducted at @0.57 V for Au$_{47}$Cd$_2$(TBBT)$_{31}$ and Au$_{44}$ and at @0.67 V for the Au NPs. Reproduced with permission.[106] Copyright 2019 Wiley-VCH.

is superior to that of other materials. Most importantly, the results confirm that the CO$_2$RR ability of Au$_{47}$Cd$_2$(TBBT)$_{31}$ is superior. Cd doped Au NCs show good performance, and other metals such as Ag,[112] Pd,[113] and Pt[114] doped Au NCs also show great performances on the CO$_2$RR.

3.5. N$_2$RR

Ammonia (NH$_3$) plays a vital role in industry and agriculture. However, the traditional industrial Haber–Bosch process is still the main way to synthesis NH$_3$, which releases many greenhouse gases and consumes a large amount of energy.[115] The N$_2$RR is believed to be a better process to produce NH$_3$. It has great advantages such as mild reaction conditions, low facility demand and environmental friendliness.[116] In recent years, Au NCs and modified Au NCs showed excellent performance on the N$_2$RR.

Ding's group prepared a Au$_{25}$–Cys–M catalyst containing transition metal ions such as Mo^{6+}, Fe^{3+}, Co^{2+}, and Ni^{2+} decorated on Au$_{25}$ nanoclusters via thiol bridging.[117] The catalyst was applied for the N$_2$RR, and it was found that it exhibited the highest faradaic efficiency (26.5%) and NH$_3$ yield (34.5 μg h^{-1} mg$_{cat}^{-1}$) in 0.1 M HCl solution. The results revealed that the Au$_{25}$–Cys–Mo catalyst could efficiently reduce N$_2$ to NH$_3$, and the synthesis provides new insight into precise fabrication of efficient N$_2$RR electrocatalysts. Jiang et al. embedded Au NCs on TiO$_2$,[118] and showed that N$_2$RR performance is much higher than the current best performance for N$_2$ fixation. The new catalyst had high and stable production yield (NH$_3$: 21.4μg h^{-1} mg$_{cat}^{-1}$, faradaic efficiency: 8.11%) and good selectivity is achieved at 0.2 V versus RHE (Fig. 13). In addition, Lu's group reported a strategy to synthesise atomically precise alloy nanoclusters,[119] where Au$_4$Pt$_2$ nanoclusters were supported on defective graphene with high activity for the N$_2$RR. Studies have shown that the active site for N$_2$ fixation is interfacial between
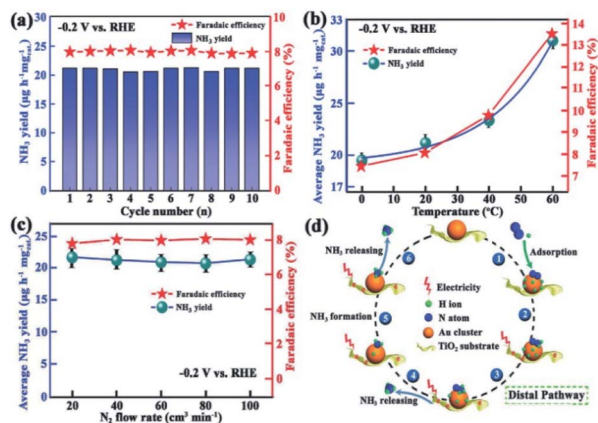
Fig. 13 (a) Yield rate of NH_3 at a potential of -0.2 V *versus* RHE; (b) yield of NH_3 (olive) and faradaic efficiency (red) against the catalytic temperature under atmospheric pressure at -0.2 V *versus* RHE; (c) yield of NH_3 (olive) and faradaic efficiency (red) against the catalytic temperature under a N_2 flow rate at -0.2 V *versus* RHE; error bars in (b) and (c) represent the standard deviations of three independent measurements of the same sample; (d) proposed pathway for the NH_3 synthesis using the Au/TiO_2. catalyst. Reproduced with permission.[118] Copyright 2017 WILEY-VCH.

the substrate and $Au_4Pt_2(SR)_6$ nanoclusters. In conclusion, these results provide valuable insight into the catalysis of the N_2RR, and the promising electrochemical performance of Au NCs lead to good prospects for the N_2RR.

4 Outlook and conclusions

In summary, atomically precise Au NCs have been studied extensively for their particular properties. They can be synthesised in various ways and applied in different electrochemical catalytic reactions to alleviate environmental and energy problems. However, more research work remains to be pursued in this field. Research and innovative synthesis methods continue to be explored for the precise number of atoms in Au NCs. For example, atomically precise Au NCs also can be produced by thermal transition and acid corrosion, which open up the potential for new electrocatalytic applications such as nitrate reduction, the sulfur dioxide oxidation reaction (SO_2OR), urea oxidation, and other oxidation reactions,[120] which will exert a profound effect on chemical and energy issues.

Due to the complexity and diversity of the electrochemical reactions, the electrocatalytic fundamentals based on Au NCs are worth unravelling. Understanding the adsorption, desorption, activation, and deactivation behaviours in the catalytic process of Au NCs will better clarify the catalytic mechanisms. In addition, the origin of the catalytically active sites is still required. The correlation between the size/composition and performance at the atomic level and the catalytic kinetic and dynamic mechanisms are still the research foci.

Finally, *in situ* characterization studies such as ESI-MS, HAADF-STEM, X-ray absorption spectroscopy and X-ray photoelectron spectroscopy can monitor the dynamics of gold

nanoclusters in real time. They can promote the understanding of the electrocatalytic reaction process of gold nanoclusters. A further study on the electrocatalytic mechanism of gold nanoclusters will make a big contribution to the development of precise atomically gold nanoclusters.

Author contributions

Q. Zhu conducted and wrote the paper. X. Huang, Y. Zeng, K. Sun, L. Zhou, Y. Liu and L. Luo finished parts of writing of the paper. S. Tian and X. Sun conceived and designed the paper. All authors contributed to the preparation of the manuscript.

Conflicts of interest

There are no conflicts to declare.

Acknowledgements

Notes and references

1 O. J. H. Chai, Z. Liu, T. Chen and J. Xie, *Nanoscale*, 2019, **11**, 20437–20448.
2 R. Jin, *Nanoscale*, 2015, **7**, 1549–1565.
3 R. Jin, *Nanoscale*, 2010, **2**, 343–362.
4 V. Sudheeshkumar, K. O. Sulaiman and R. W. J. Scott, *Nanoscale Adv.*, 2020, **2**, 55–69.
5 S. Wang, H. Yu and M. Zhu, *Sci. China: Chem.*, 2015, **59**, 206–208.
6 R. Jin, C. Zeng, M. Zhou and Y. Chen, *Chem. Rev.*, 2016, **116**, 10346–10413.
7 Y. Yu, X. Chen, Q. Yao, Y. Yu, N. Yan and J. Xie, *Chem. Mater.*, 2013, **25**, 946–952.
8 K. Pyo, V. D. Thanthirige, S. Y. Yoon, G. Ramakrishna and D. Lee, *Nanoscale*, 2016, **8**, 20008–20016.
9 Y. Wang and T. Burgi, *Nanoscale Adv.*, 2021, **3**, 2710–2727.
10 Y. Levi-Kalisman, P. D. Jadzinsky, N. Kalisman, H. Tsunoyama, T. Tsukuda, D. A. Bushnell and R. D. Kornberg, *J. Am. Chem. Soc.*, 2011, **133**, 2976–2982.
11 Z. Lei, Z. J. Guan, X. L. Pei, S. F. Yuan, X. K. Wan, J. Y. Zhang and Q. M. Wang, *Chem.–Eur. J.*, 2016, **22**, 11156–11160.
12 G. Deng, S. Malola, J. Yan, Y. Han, P. Yuan, C. Zhao, X. Yuan, S. Lin, Z. Tang, B. K. Teo, H. Hakkinen and N. Zheng, *Angew. Chem., Int. Ed.*, 2018, **57**, 3421–3425.
13 Y. Lu and W. Chen, *Chem. Soc. Rev.*, 2012, **41**, 3594–3623.
14 B. Yang, H. Wu and L. Zhao, *Chem. Commun.*, 2021, **57**, 5770–5773.

15 H. Shen, S. Xiang, Z. Xu, C. Liu, X. Li, C. Sun, S. Lin, B. K. Teo and N. Zheng, *Nano Res.*, 2020, **13**, 1908–1911.

16 S. Antonello, N. V. Perera, M. Ruzzi, J. A. Gascon and F. Maran, *J. Am. Chem. Soc.*, 2013, **135**, 15585–15594.

17 B. Kumar, T. Kawawaki, N. Shimizu, Y. Imai, D. Suzuki, S. Hossain, L. V. Nair and Y. Negishi, *Nanoscale*, 2020, **12**, 9969–9979.

18 M. Brust, M. Walker, D. Bethell, D. J. Schiffrin and R. Whyman, *J. Chem. Soc., Chem. Commun.*, 1994, 801–802.

19 S. Tian, L. Liao, J. Yuan, C. Yao, J. Chen, J. Yang and Z. Wu, *Chem. Commun.*, 2016, **52**, 9873–9876.

20 X. He, C. Y. Gao, M. X. Wang and L. Zhao, *Chem. Commun.*, 2012, **48**, 10877–10879.

21 C. Zeng, T. Li, A. Das, N. L. Rosi and R. Jin, *J. Am. Chem. Soc.*, 2013, **135**, 10011–10013.

22 S. Tian, C. Yao, L. Liao, N. Xia and Z. Wu, *Chem. Commun.*, 2015, **51**, 11773–11776.

23 T. Kawawaki and Y. Negishi, *Nanomaterials*, 2020, **10**, 238.

24 C. Li, O. J. H. Chai, Q. Yao, Z. Liu, L. Wang, H. Wang and J. Xie, *Mater. Horiz.*, 2021, **8**, 1657–1682.

25 L. Liu and A. Corma, *Chem. Rev.*, 2018, **118**, 4981–5079.

26 X. Kang, Y. Li, M. Zhu and R. Jin, *Chem. Soc. Rev.*, 2020, **49**, 6443–6514.

27 X. Dou, X. Wang, S. Qian, N. Liu and X. Yuan, *Nanoscale*, 2020, **12**, 19855–19860.

28 M. Brust, J. Fink, D. Bethell, D. J. Schiffrin and C. Kiely, *J. Chem. Soc., Chem. Commun.*, 1995, 1655–1656.

29 A. Das, T. Li, K. Nobusada, C. Zeng, N. L. Rosi and R. Jin, *J. Am. Chem. Soc.*, 2013, **135**, 18264–18267.

30 O. Toikkanen, V. Ruiz, G. Rönnholm, N. Kalkkinen, P. Liljeroth and B. M. Quinn, *J. Am. Chem. Soc.*, 2008, **130**, 11049–11055.

31 Y. Yang and S. Chen, *Nano Lett.*, 2003, **3**, 75–79.

32 R. Jin, H. Qian, Z. Wu, Y. Zhu, M. Zhu, A. Mohanty and N. Garg, *J. Phys. Chem. Lett.*, 2010, **1**, 2903–2910.

33 D. Liu, W. Du, S. Chen, X. Kang, A. Chen, Y. Zhen, S. Jin, D. Hu, S. Wang and M. Zhu, *Nat. Commun.*, 2021, **12**, 778.

34 H. Qian, W. T. Eckenhoff, M. E. Bier, T. Pintauer and R. Jin, *Inorg. Chem.*, 2011, **50**, 10735–10739.

35 X. Liu, W. W. Xu, X. Huang, E. Wang, X. Cai, Y. Zhao, J. Li, M. Xiao, C. Zhang, Y. Gao, W. Ding and Y. Zhu, *Nat. Commun.*, 2020, **11**, 3349.

36 H. Qian, Y. Zhu and R. Jin, *ACS Nano*, 2009, **3**, 3795–3803.

37 C. Zeng, Y. Chen, G. Li and R. Jin, *Chem. Mater.*, 2014, **26**, 2635–2641.

38 C. Liu, J. Lin, Y. Shi and G. Li, *Nanoscale*, 2015, **7**, 5987–5990.

39 H. Qian, D. E. Jiang, G. Li, C. Gayathri, A. Das, R. R. Gil and R. Jin, *J. Am. Chem. Soc.*, 2012, **134**, 16159–16162.

40 Y. Yu, Z. Luo, Y. Yu, J. Y. Lee and J. Xie, *ACS Nano*, 2012, **6**, 7920–7927.

41 Z. Luo, V. Nachammai, B. Zhang, N. Yan, D. T. Leong, D. E. Jiang and J. Xie, *J. Am. Chem. Soc.*, 2014, **136**, 10577–10580.

42 Y. Cao, V. Fung, Q. Yao, T. Chen, S. Zang, D. E. Jiang and J. Xie, *Nat. Commun.*, 2020, **11**, 5498.

43 G. B. Hwang, G. Wu, J. Shin, L. Panariello, V. Sebastian, K. Karu, E. Allan, A. Gavriilidis and I. P. Parkin, *ACS Appl. Mater. Interfaces*, 2020, **12**, 49021–49029.

44 Y. Yu, Q. Yao, T. Chen, G. X. Lim and J. Xie, *J. Phys. Chem. C*, 2016, **120**, 22096–22102.

45 G. Li, H. Abroshan, C. Liu, S. Zhuo, Z. Li, Y. Xie, H. J. Kim, N. L. Rosi and R. Jin, *ACS Nano*, 2016, **10**, 7998–8005.

46 X. Meng, Z. Liu, M. Zhu and R. Jin, *Nanoscale Res. Lett.*, 2012, **7**, 277.

47 S. H. Li, X. Liu, W. Hu, M. Chen and Y. Zhu, *J. Phys. Chem. A*, 2020, **124**, 6061–6067.

48 C. E. Briant, K. P. Hall, A. C. Wheeler and D. M. P. Mingos, *J. Chem. Soc., Chem. Commun.*, 1984, 248–250.

49 Y. Shichibu, K. Suzuki and K. Konishi, *Nanoscale*, 2012, **4**, 4125–4129.

50 S. S. Zhang, R. D. Senanayake, Q. Q. Zhao, H. F. Su, C. M. Aikens, X. P. Wang, C. H. Tung, D. Sun and L. S. Zheng, *Dalton Trans.*, 2019, **48**, 3635–3640.

51 X. Yuan, B. Zhang, Z. Luo, Q. Yao, D. T. Leong, N. Yan and J. Xie, *Angew. Chem., Int. Ed.*, 2014, **53**, 4623–4627.

52 X. K. Wan, Z. J. Guan and Q. M. Wang, *Angew. Chem., Int. Ed.*, 2017, **56**, 11494–11497.

53 Z. Qin, D. Zhao, L. Zhao, Q. Xiao, T. Wu, J. Zhang, C. Wan and G. Li, *Nanoscale Adv.*, 2019, **1**, 2529–2536.

54 Y. Bao, C. Zhong, D. Vu, J. Temirov, R. Dyer and J. Martinez, *J. Phys. Chem. C*, 2007, **111**, 12194–12198.

55 A. Retnakumari, S. Setua, D. Menon, P. Ravindran, H. Muhammed, T. Pradeep, S. Nair and M. Koyakutty, *Nanotechnology*, 2010, **21**, 055103.

56 X. Yang, M. Shi, R. Zhou, X. Chen and H. Chen, *Nanoscale*, 2011, **3**, 2596–2601.

57 F. Bertorelle, I. Russier-Antoine, C. Comby-Zerbino, F. Chirot, P. Dugourd, P. F. Brevet and R. Antoine, *ACS Omega*, 2018, **3**, 15635–15642.

58 Z. Wei, W. Jiang, Z. Bai, Z. Lian, Z. Wang and F. Song, *Eur. Phys. J. D*, 2017, **71**, 237.

59 S. Hossain, W. Kurashige, S. Wakayama, B. Kumar, L. V. Nair, Y. Niihori and Y. Negishi, *J. Phys. Chem. C*, 2016, **120**, 25861–25869.

60 Z. Wu and R. Jin, *Nano Lett.*, 2010, **10**, 2568–2573.

61 S. Malola, L. Lehtovaara, S. Knoppe, K. J. Hu, R. E. Palmer, T. Burgi and H. Hakkinen, *J. Am. Chem. Soc.*, 2012, **134**, 19560–19563.

62 Y. Negishi, W. Kurashige and U. Kamimura, *Langmuir*, 2011, **27**, 12289–12292.

63 T. W. Ni, M. A. Tofanelli, B. D. Phillips and C. J. Ackerson, *Inorg. Chem.*, 2014, **53**, 6500–6502.

64 Y. Song, H. Abroshan, J. Chai, X. Kang, H. J. Kim, M. Zhu and R. Jin, *Chem. Mater.*, 2017, **29**, 3055–3061.

65 Y. Wang, B. Nieto-Ortega and T. Burgi, *Chem. Commun.*, 2019, **55**, 14914–14917.

66 S. Knoppe, A. C. Dharmaratne, E. Schreiner, A. Dass and T. Bürgi, *J. Am. Chem. Soc.*, 2010, **132**, 16783–16789.

67 Y. Niihori, M. Eguro, A. Kato, S. Sharma, B. Kumar, W. Kurashige, K. Nobusada and Y. Negishi, *J. Phys. Chem. C*, 2016, **120**, 14301–14309.

68 R. Zhou, M. Shi, X. Chen, M. Wang and H. Chen, *Chemistry*, 2009, **15**, 4944–4951.

69 M. A. Habeeb Muhammed, S. Ramesh, S. S. Sinha, S. K. Pal and T. Pradeep, *Nano Res.*, 2010, **1**, 333–340.

70 H. Duan and S. Nie, *J. Am. Chem. Soc.*, 2007, **129**, 2412–2413.

71 W. Guo, J. Yuan and E. Wang, *Chem. Commun.*, 2012, **48**, 3076–3078.

72 D. Bain, S. Maity, T. Debnath, A. K. Das and A. Patra, *Mater. Res. Express*, 2019, **6**, 124004.

73 Z. Wu, *Angew. Chem., Int. Ed.*, 2012, **51**, 2934–2938.

74 M. Zhu, P. Wang, N. Yan, X. Chai, L. He, Y. Zhao, N. Xia, C. Yao, J. Li, H. Deng, Y. Zhu, Y. Pei and Z. Wu, *Angew. Chem., Int. Ed.*, 2018, **57**, 4500–4504.

75 C. Yao, J. Chen, M. B. Li, L. Liu, J. Yang and Z. Wu, *Nano Lett.*, 2015, **15**, 1281–1287.

76 C. Yao, Y. J. Lin, J. Yuan, L. Liao, M. Zhu, L. H. Weng, J. Yang and Z. Wu, *J. Am. Chem. Soc.*, 2015, **137**, 15350–15353.

77 S. Zhuang, D. Chen, L. Liao, Y. Zhao, N. Xia, W. Zhang, C. Wang, J. Yang and Z. Wu, *Angew. Chem., Int. Ed.*, 2020, **59**, 3073–3077.

78 M.-B. Li, S.-K. Tian and Z. Wu, *Chin. J. Chem.*, 2017, **35**, 567–571.

79 S. Wang, Y. Song, S. Jin, X. Liu, J. Zhang, Y. Pei, X. Meng, M. Chen, P. Li and M. Zhu, *J. Am. Chem. Soc.*, 2015, **137**, 4018–4021.

80 H. Tsunoyama, H. Sakurai and T. Tsukuda, *Chem. Phys. Lett.*, 2006, **429**, 528–532.

81 Q. Yao, X. Yuan, V. Fung, Y. Yu, D. T. Leong, D. E. Jiang and J. Xie, *Nat. Commun.*, 2017, **8**, 927.

82 H. Qian, C. Liu and R. Jin, *Sci. China: Chem.*, 2012, **55**, 2359–2365.

83 C. Zeng, H. Qian, T. Li, G. Li, N. L. Rosi, B. Yoon, R. N. Barnett, R. L. Whetten, U. Landman and R. Jin, *Angew. Chem., Int. Ed.*, 2012, **51**, 13114–13118.

84 A. Baksi, T. Pradeep, B. Yoon, C. Yannouleas and U. Landman, *Chemphyschem*, 2013, **14**, 1272–1282.

85 T. Tsukamoto, T. Kambe, A. Nakao, T. Imaoka and K. Yamamoto, *Nat. Commun.*, 2018, **9**, 3873.

86 P. Lv, L. Qiu, C. Zhao, G. Fang, J. Liu and S. Wang, *ChemNanoMat*, 2018, 158–162, DOI: 10.1002/cnma.201800527.

87 M. Shao, Q. Chang, J. P. Dodelet and R. Chenitz, *Chem. Rev.*, 2016, **116**, 3594–3657.

88 L. Wang, Z. Tang, W. Yan, H. Yang, Q. Wang and S. Chen, *ACS Appl. Mater. Interfaces*, 2016, **8**, 20635–20641.

89 Y. Lu, Y. Jiang, X. Gao and W. Chen, *Chem. Commun.*, 2014, **50**, 8464–8467.

90 Q. Wang, L. Wang, Z. Tang, F. Wang, W. Yan, H. Yang, W. Zhou, L. Li, X. Kang and S. Chen, *Nanoscale*, 2016, **8**, 6629–6635.

91 L. Sumner, N. A. Sakthivel, H. Schrock, K. Artyushkova, A. Dass and S. Chakraborty, *J. Phys. Chem. C*, 2018, **122**, 24809–24817.

92 C. Cai, S. Han, Q. Wang and M. Gu, *ACS Nano*, 2019, **13**, 8865–8871.

93 Y. Zhou and H. C. Zeng, *J. Phys. Chem. C*, 2016, **120**, 29348–29357.

94 T. Kawawaki, A. Ebina, Y. Hosokawa, S. Ozaki, D. Suzuki, S. Hossain and Y. Negishi, *Small*, 2021, **17**, 2005328.

95 Y. Wang, P. Gao, X. Wang, J. Huo, L. Li, Y. Zhang, A. A. Volinsky, P. Qian and Y. Su, *Phys. Chem. Chem. Phys.*, 2018, **20**, 14545–14556.

96 S. Zhao, R. Jin, H. Abroshan, C. Zeng, H. Zhang, S. D. House, E. Gottlieb, H. J. Kim, J. C. Yang and R. Jin, *J. Am. Chem. Soc.*, 2017, **139**, 1077–1080.

97 S. Youk, J. Hwang, S. Lee, M. S. Kim and J. Lee, *Small Methods*, 2018, **3**, 1800293.

98 Z. Zhuang, Y. Wang, C. Q. Xu, S. Liu, C. Chen, Q. Peng, Z. Zhuang, H. Xiao, Y. Pan, S. Lu, R. Yu, W. C. Cheong, X. Cao, K. Wu, K. Sun, Y. Wang, D. Wang, J. Li and Y. Li, *Nat. Commun.*, 2019, **10**, 4875.

99 S. Liu, Z. Hu, Y. Wu, J. Zhang, Y. Zhang, B. Cui, C. Liu, S. Hu, N. Zhao, X. Han, A. Cao, Y. Chen, Y. Deng and W. Hu, *Adv. Mater.*, 2020, **32**, 2006034.

100 Y. Gu, A. Wu, Y. Jiao, H. Zheng, X. Wang, Y. Xie, L. Wang, C. Tian and H. Fu, *Angew. Chem., Int. Ed.*, 2021, **60**, 6673–6681.

101 K. Kwak, W. Choi, Q. Tang, M. Kim, Y. Lee, D. E. Jiang and D. Lee, *Nat. Commun.*, 2017, **8**, 14723.

102 W. Choi, G. Hu, K. Kwak, M. Kim, D.-e. Jiang, J.-P. Choi and D. Lee, *ACS Appl. Mater. Interfaces*, 2018, **10**, 44645–44653.

103 G. Hu, Q. Tang, D. Lee, Z. Wu and D.-e. Jiang, *Chem. Mater.*, 2017, **29**, 4840–4847.

104 S. Zhao, R. Jin, Y. Song, H. Zhang, S. D. House, J. C. Yang and R. Jin, *Small*, 2017, **13**, 1701519.

105 Y. Du, J. Xiang, K. Ni, Y. Yun, G. Sun, X. Yuan, H. Sheng, Y. Zhu and M. Zhu, *Inorg. Chem. Front.*, 2018, **5**, 2948–2954.

106 S. Zhuang, D. Chen, L. Liao, Y. Zhao, N. Xia, W. Zhang, C. Wang, J. Yang and Z. Wu, *Angew. Chem., Int. Ed.*, 2020, **59**, 3073–3077.

107 N. Austin, S. Zhao, J. R. McKone, R. Jin and G. Mpourmpakis, *Catal. Sci. Technol.*, 2018, **8**, 3795–3805.

108 S. Li, A. V. Nagarajan, D. R. Alfonso, M. Sun, D. R. Kauffman, G. Mpourmpakis and R. Jin, *Angew. Chem., Int. Ed.*, 2021, **60**, 6351–6356.

109 D. R. Kauffman, D. Alfonso, C. Matranga, H. Qian and R. Jin, *J. Am. Chem. Soc.*, 2012, **134**, 10237–10243.

110 D. Yang, W. Pei, S. Zhou, J. Zhao, W. Ding and Y. Zhu, *Angew. Chem., Int. Ed.*, 2020, **59**, 1919–1924.

111 H. Seong, V. Efremov, G. Park, H. Kim, J. S. Yoo and D. Lee, *Angew. Chem., Int. Ed.*, 2021, **60**, 14563–14570.

112 S. Zhao, R. Jin and R. Jin, *ACS Energy Lett.*, 2018, **3**, 452–462.

113 S. Li, D. Alfonso, A. V. Nagarajan, S. D. House, J. C. Yang, D. R. Kauffman, G. Mpourmpakis and R. Jin, *ACS Catal.*, 2020, **10**, 12011–12016.

114 K. Kwak and D. Lee, *Acc. Chem. Res.*, 2019, **52**, 12–22.

115 Y. Liu, L. Huang, X. Zhu, Y. Fang and S. Dong, *Nanoscale*, 2020, **12**, 1811–1816.

116 C. Chen, C. Liang, J. Xu, J. Wei, X. Li, Y. Zheng, J. Li, H. Tang and J. Li, *Electrochim. Acta*, 2020, **335**, 135708.

117 Y. Tan, L. Yan, C. Huang, W. Zhang, H. Qi, L. Kang, X. Pan, Y. Zhong, Y. Hu and Y. Ding, *Small*, 2021, **17**, 2100372.

118 M. M. Shi, D. Bao, B. R. Wulan, Y. H. Li, Y. F. Zhang, J. M. Yan and Q. Jiang, *Adv. Mater.*, 2017, **29**, 1606550.

119 C. Yao, N. Guo, S. Xi, C. Q. Xu, W. Liu, X. Zhao, J. Li, H. Fang, J. Su, Z. Chen, H. Yan, Z. Qiu, P. Lyu, C. Chen, H. Xu, X. Peng, X. Li, B. Liu, C. Su, S. J. Pennycook,

C. J. Sun, J. Li, C. Zhang, Y. Du and J. Lu, *Nat. Commun.*, 2020, **11**, 4389.

120 S. Tian, Y. Cao, T. Chen, S. Zang and J. Xie, *Chem. Commun.*, 2020, **56**, 1163–1174.